RSC Advances

ROYAL SOCIETY OF CHEMISTRY

www.rsc.org/advances

Kinetic and mechanistic investigations of thermal decomposition of methyl-substituted cycloalkyl radicals

Long Chen [a], Wenliang Wang [a,*], Weina Wang [a], Chunying Li [b], Fengyi Liu [a], Jian Lü [b,*]

[a] School of Chemistry and Chemical Engineering, Key Laboratory for Macromolecular Science of Shaanxi Province, Shaanxi Normal University, Xi'an, Shaanxi 710062, People's Republic of China
[b] Xi'an Modern Chemistry Research Institute, Xi'an 710065, People's Republic of China

Abstract: A systematically theoretical study on the thermal decomposition of 2-Me-cyclobutyl, 2-Me-cyclopentyl and 2-Me-cyclohexyl radicals is performed using the high-level *ab initio* CBS-QB3 and CCSD(T) quantum chemical calculations. The calculation reveals that the detailed reaction mechanism of the thermal decomposition of these cyclic alkyl radicals incorporates the ring opening, vinyl rearrangements (exocyclization), beta-site C-C bond cleavage and H-elimination processes. The standard reaction enthalpies ($\Delta_r H^0_{298}$) and Gibbs free energies ($\Delta_r G^0_{298}$) for each elementary reaction involved in 2-Me-cyclohexyl radical reactive system are also determined with composite CBS-QB3 method. All investigated vinyl rearrangements reactions are exothermic and spontaneous, while the ring opening, C-C bond scission and H-elimination processes are endothermic and nonspontaneous. Among all investigated elementary reactions, the exocyclization processes are kinetically accessible and readily proceeds (due to their significantly lower barrier and high exothermic). Compared with the barrier heights for the distinct vinyl rearrangement pathways in these cyclic alkyl radicals, it can be found that they decrease in the order of 1,3- > 1,2- > 1,4-vinyl transfer. The branching ratios are evaluated at different temperatures on the basis of the quasi-steady state approximation (QSSA). The calculated result shows that the 1,2-, 1,3- and 1,4-vinyl rearrangement reactions are advantaged at low temperature, while the formations of cycloalkene are favoured at high temperature.

Keywords: Cycloalkyl radicals; Reaction mechanisms; Transition state theory; Rate

Corresponding authors. Tel: +86-29-81530815, Fax: +86-29-81530727.
e-mail: wlwang@snnu.edu.cn (W. L. Wang), lujian204@263.net (J. Lü).

coefficients; Branching ratios

1. Introduction

Many studies have been performed on the reactions of straight and branched-chain alkanes in a wide range of temperatures and pressures,[1-3] while the chemistry of cyclic hydrocarbons has been investigated to a much lesser extent.[4,5] Cyclic hydrocarbons, particularly cycloalkanes, constitute an important source in practical fuels.[6] Cycloalkyl radicals are key intermediate species in the thermal decomposition processes of cycloalkanes.[4] They result from the initial steps of hydrocarbon pyrolysis through the C-H bond fission or abstraction H-atom reactions by mean of small chemical species (such as H, OH, CH_3 radicals etc.) attack on parent molecules. Herein, the mechanistic and kinetic properties of cycloalkyl radicals are important to further improve our understanding of the thermal decomposition processes of hydrocarbons.

To date, no experimental evidence on the thermal decomposition routes of cyclic alkyl radical has been reported. Such low stability, short lifetime and highly reactive radicals are excessively difficult to be determined and characterized in the gas phase experimentally. In 2006, Orme et al[5] investigated the oxidation and pyrolysis of methylcyclohexane (MCH) at 1200-2100 K and 1.0, 2.0, and 4.0 atm, by means of high temperature shock tube and flow reactor. The author found that the major pyrolysis products contain methane (CH_4), ethylene (C_2H_4), propene (C_3H_6), 1,3-butadiene (1,3-C_4H_6) and isoprene (C_5H_8). And they also proposed a detailed chemical kinetic mechanism on the pyrolysis of MCH. Similar product distributions were also drawn in Zeppieri et al studies[7] that the high temperature pyrolysis of pure MCH and MCH/toluene blends are performed in the princeton turbulent flow reactor. All of these works have provided insight into the thermal decomposition behavior of cycloalkanes and their radicals. However, the estimated rate coefficients of elementary reactions in Orme's study[5] are not accurate adequately, because they adopted that the rate coefficients of chemical reactions of similar nature are equal to those reported by Curran et al for n-heptane[8] and isooctane[9] oxidation. Moreover, the

dominant reaction pathways have not been mentioned during the processes of MCH and its radical pyrolysis.

To the best of our knowledge, the detailed reaction mechanisms of second reactions of cycloalkyl radicals have not been reported so far. Sirjean et al[4] studied the beta site C-C and C-H bonds breaking reactions for cyclic alkyl radicals from three-membered to seven-membered rings, with and without a lateral alkyl chain by means of quantum chemical calculations at the CBS-QB3 level of theory. It is concluded that the increase of the activation energy as the π bond is being formed in the ring in contrast to the cases in which the π bond is formed on the side chain. Sirjean et al[6] also investigated the gas phase unimolecular decomposition of cyclobutane, cyclopentane and cyclohexane molecules, and considered the formation of biradical species. The result showed that the main part of ring strain energies contained in the cyclic reactants is removed from the cycloalkanes to the transition states. Wang et al[10] studied the kinetics of a series of homoallylic/homobenzylic rearrangement reactions under combustion conditions. They mainly considered the 1,2-, 1,3- and 1,4-vinyl/phenyl migration for homoallylic and homobenzylic radicals, and compared theirs product yield. The calculation indicated that the 1,2-vinyl/phenyl migration is particularly important for the kinetics of unimolecular reactions of homoallylic radicals, whereas the 1,3- and 1,4-vinyl/phenyl migration channel play an insignificant role under combustion conditions. All of these works provide useful information for investigating the pyrolysis of cyclic alkyl radicals. Unfortunately, the vinyl migration process of cycloalkyl radicals is neglected in Sirjean's study,[4] which is an very important reaction type in pyrolysis process of hydrocarbon, especially at low temperature. Moreover, they merely considered the initial ring opening steps, not mentioned the second reactions of the radicals formed and not compared their relative importance.

In the recent work, we perform systemically theoretical investigations about the thermal decomposition of 2-Me-cyclobutyl, 2-Me-cyclopentyl and 2-Me-cyclohexyl radicals at the high-level composite CBS-QB3 *ab initio* and the coupled-cluster CCSD(T) approaches. The calculations are laid out as follows: firstly, the pyrolysis

mechanism of these radicals, including the ring opening, vinyl rearrangements (exocyclization), the beta site C-C bond cleavage and H-elimination reactions, are explored. Secondly, the standard reaction enthalpies ($\Delta_r H^0_{298}$) and Gibbs free energies ($\Delta_r G^0_{298}$) for every elementary reaction are calculated. Thirdly, the high-pressure limit (HPL) rate coefficients of conventional transition state theory for individual elementary reaction are determined at 500-2500 K. Finally, the branching ratios of thermal decomposition of these radicals are predicted at different temperatures. The computational results, along with detailed discussions, will be presented in Section 3 and main conclusions will be drawn in Section 4.

2. Computational approach

All the electronic structure calculations that are discussed in the present investigation are carried out using the Gaussian 09 quantum chemistry code.[11] The geometry optimizations for all species are performed with an unrestricted B3LYP functional, which has been successfully applied to the study of organic molecules.[12] Moreover, the effectiveness of B3LYP in modeling radical reactions has been proposed in previous studies.[13-16] The basis set 6-311G(2d,d,p), which is reasonably accurate and computationally affordable, is adopted for all stationary points calculations. The vibrational frequency calculations are performed to verify that the optimized structures are either real local minima (no imaginary frequencies) or first order saddle points (just one imaginary frequencies) and to estimate the thermodynamic quantities. Intrinsic reaction coordinate (IRC) calculations[17-20] are traced at the same level of theory to confirm that the located transition state structures indeed connect to the designated reactants and products. Then, to obtain reliable energies of each species on the potential energy surface (PES), the single point calculations are performed at the CBS-QB3 and CCSD(T) levels of theory. The composite CBS-QB3 methodology involves a five-step calculation: (i) a geometry optimization and a frequency calculation (scaled by 0.99 as recommended by Montgomery et al[21]) at the B3LYP/6-311G(2d,d,p) level of theory[22]; (ii) CCSD(T)/6-31+G(d') energy corrections; (iii) MP4SDQ/CBSB4 (CBSB4 =

6-31+G(d(f),p)) energy; (iv) MP2/CBSB3 (CBSB3 = 6-311+G(3d2f,2df,2p)) energy; (v) a complete basis set (CBS) extrapolation to correct the total energy.[14,23,24] The CBS-QB3 approach is chosen because it gives adequately accurate energies for C/H/O system, with a standard deviation of about 1.5 kcal·mol^{-1}, and it is less computationally cost than the more recent and accurate ones, as G4.[15] The coupled-cluster approach CCSD(T), involving single and double substitutions including perturbative corrections for the triple excitations,[25] is used to obtain more reliable energies based on the B3LYP geometries. T_1 diagnostics in the CCSD(T) energy calculations are considered to evaluate the reliability of the calculations for all stationary points involved in the above mentioned reaction mechanisms. They are all less than critical value 0.02 for the singlet species (see Table S1-S3), revealing that the CCSD(T) method employed provides an adequate description of the wave function.[26] The theoretical rate coefficients of conventional transition state theory for every elementary reaction are estimated over the temperature range of 500-2500 K. Tunneling effects are contained on the base of an one-dimensional asymmetric Eckart transmission factor.[27-29]

$$k(T) = \kappa(T)\sigma \frac{k_B T}{h} \frac{Q^{\neq}(T)}{Q_A(T)Q_B(T)} \exp(-E_a / RT) \quad (1)$$

where $\kappa(T)$ is the asymmetric Eckart tunneling factor, σ is reaction symmetry number, k_B is the Boltzmann constant. h is the Planck constant, $Q^{\neq}(T)$ is the partition function for the transition state, $Q_A(T)$ and $Q_B(T)$ are the partition functions for the reactants and E_a is the activation energy barrier. The total molar partition function includes translation (Q_{trans}), vibration (Q_{vib}), rotation (Q_{rot}), electronic (Q_{ele}) and torsional (Q_{tor}) partition functions ($Q = Q_{trans}Q_{vib}Q_{rot}Q_{ele}Q_{tor}$).[30] The one-dimensional hindered rotor (1D-HR) partition function Q_{tor} is calculated by the following eq 2.[31]

$$Q_{tor} = \frac{1}{\sigma'} \sum_i \exp(-\frac{\varepsilon_i}{k_B T}) \quad (2)$$

where σ' is symmetry number associated with that rotation, ε_i is the energy. The internal rotations of both reactant and transition state is investigated using the 1-D hindered rotor treatment. The hindrance potential for an internal rotor is obtained by

relaxed potential energy scan with the step of 12° at the B3LYP/6-311G(2d,d,p) level. The quasi-steady-state approximation (QSSA) is employed to induce the overall rate coefficients. The rate coefficients are fitted to the modified three parameters Arrhenius expression:

$$k = A \times T^n \times \exp(-E_a / \mathrm{R}T) \quad (3)$$

The kinetic calculations are evaluated by implementing VKLab program.[32]

3. Results and discussion

The global flux diagram for the detailed reaction mechanism of 2-Me-cyclobutyl, 2-Me-cyclopentyl and 2-Me-cyclohexyl radicals is drawn in Scheme 1. As shown in Scheme 1, the detailed mechanism includes mainly the ring opening, vinyl rearrangements (exocyclization), beta C-C bond dissociation and H-elimination processes. The geometrical parameters for all stationary points involved in the 2-Me-cyclohexyl radical reaction system at the B3LYP/6-311G(2d,d,p) level together with the available experimental values, are depicted in Fig. 1. The expectation values of $<S^2>$ for all species are listed in Table S1-S3, after spin annihilation, the value for the open-shell systems is very close to the ideal value of 0.7500, indicating it can be negligible at the above depicted computation level. The standard reaction enthalpies ($\Delta_r H^{\circ}_{298}$) and Gibbs free energies ($\Delta_r G^{0}_{298}$) for every elementary reaction in Table 1 are estimated at the CBS-QB3 level, and are compared with the available literature values. The PESs for these cycloalkyl radicals reactions at the CBS-QB3 and CCSD(T) levels of theory, respectively, are constructed in Fig. 2-4. The full structural descriptions of all transition states are displayed in Fig. S1-S3 in the Supporting Information. The modified three parameter Arrhenius expressions for each elementary reaction rate coefficient in Table 2 are listed. The branching ratio of these radicals pyrolysis is calculated in Fig. 7 over the temperature range of 500-2500 K.

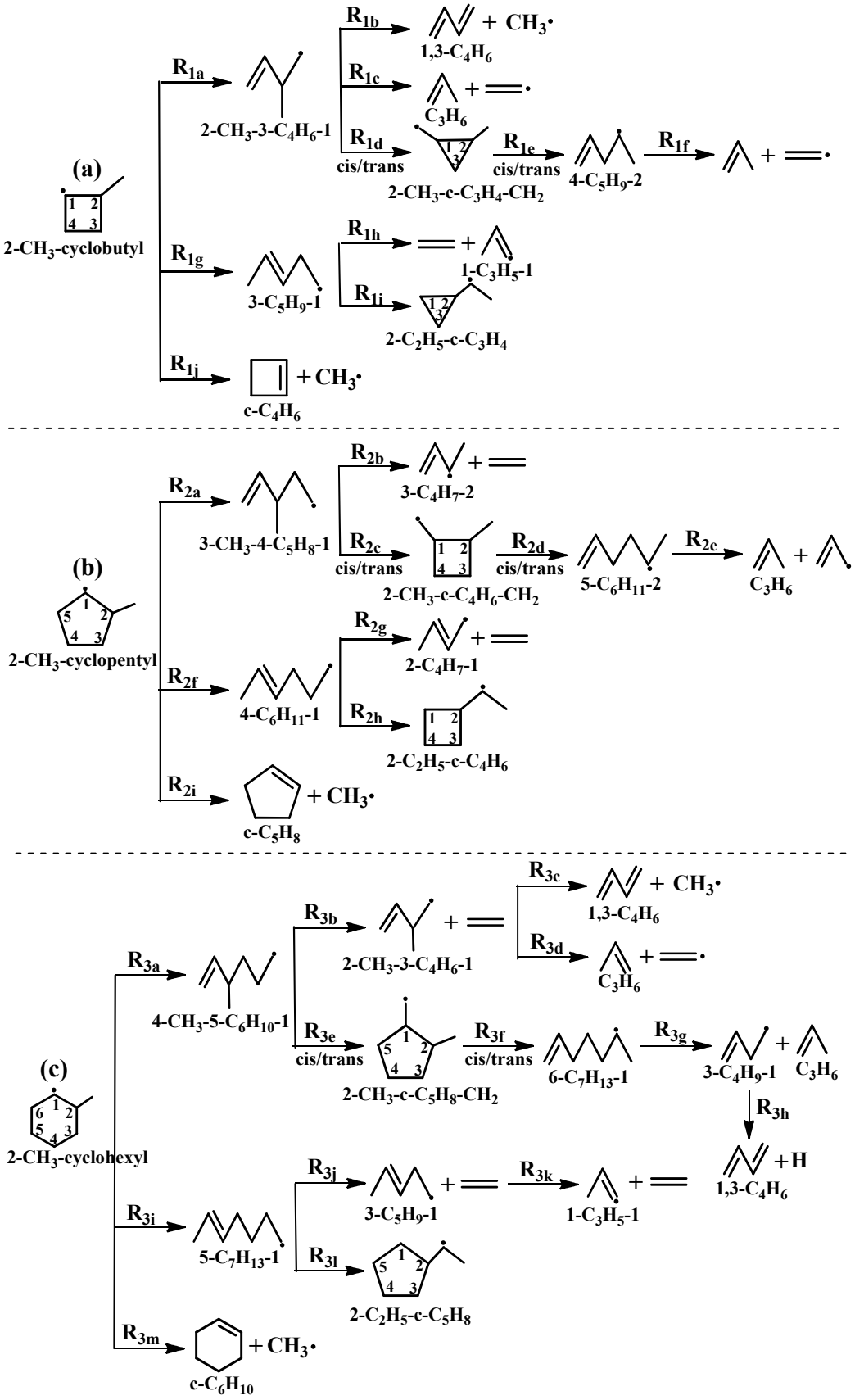

Scheme 1 The global flux diagram for the pyrolysis of 2-Me-cyclobutyl, 2-Me-cyclopentyl and 2-Me-cyclohexyl radicals (the prefix and postfix of the number represent the site of double bond and radical, respectively)

3.1 Geometrical parameters and thermodynamic properties

Fig. 1 details the optimized geometries of all stationary points involved in 2-Me-cyclohexyl radical at the B3LYP/6-311G(2d,d,p) level of theory, as well as available experimental values. The NIST Standard Reference Database (http://cccbdb.nist.gov) values are chosen as a reference to assess the accuracy of the computational methodology employed through comparing the deviation of the bond lengths and angles.

As shown in Fig. 1, the calculated values of the bond lengths and angles are in good agreement with available experimental ones. The mean average deviations of bond lengths and bond angles between the calculated and experimental values are 0.01 Å and 0.87°, respectively. The largest deviations of bond lengths and bond angles is 0.02 Å for C=C bond in C_3H_6 molecule and 1.43° for ∠C-C-C angle in 1,3-C_4H_6 molecule. These calculated results reveal that the method employed is suitable to describe the geometries in the reaction mechanisms of the title reaction system.

The standard reaction enthalpies ($\Delta_r H^0_{298}$) and Gibbs free energies ($\Delta_r G^0_{298}$) are evaluated under the condition of 298 K and 1 atm.[16,33] The enthalpies of formations for partial species with available experimental values come from NIST Chemistry Webbook (http://webbook.nist.gov/chemistry) or references.[4,5] The $\Delta_r H^0_{298}$ and $\Delta_r G^0_{298}$ for each elementary reaction involved in 2-Me-cyclohexyl radical are calculated at the CBS-QB3 model chemistry, and the results are listed in Table 1.

As is readily apparent from Table 1, the calculated reaction enthalpies are in good agreement with available literature ones for reaction R_{3c}, R_{3d}, R_{3h}, R_{3j} and R_{3m}. The largest deviation is equal to 1.36 kcal·mol^{-1} (R_{3j}), suggesting the present CB3-QB3 approach is reasonable to discuss the thermodynamic property of the title reaction system. The conclusion is also supported by the pervious literature reported[24] that CBS-QB3 reproduces the experimental results and recommends as a reference

where experimental values are not available. The exocyclization reactions ($R_{3e\text{-}cis}$, $R_{3e\text{-}trans}$ and R_{3l}) are exothermic and spontaneous with releasing heat ~ 16 kcal·mol^{-1}, whereas the ring opening, H-elimination and C-C bond scission processes are endothermic and nonspontaneous with absorbing heat 14-34 kcal·mol^{-1}. The reaction exothermicities for the distinct exocyclization channels are almost equivalent in our system studied.

In summary, the CBS-QB3 approach used provides adequately accurate geometrical parameters and thermodynamic values in the title reaction system. The exocyclization reactions are exothermic and spontaneous, while the ring opening, C-C bond scission and H-elimination processes are endothermic and nonspontaneous.

3.2 Reaction mechanisms

The radical chain mechanism is nowadays accepted for the pyrolysis of hydrocarbons.[34] According to this reactive mechanism, the 2-Me-cyclohexyl, 2-Me-cyclopentyl and 2-Me-cyclobutyl radicals undergoes the ring opening, exocyclization, beta C-C bond scission and H-elimination processes (Scheme 1). Fig. 2-4 present the PESs of the thermal decomposition of these radicals at the CBS-QB3 and CCSD(T) levels of theory. The full structural descriptions for all transition states are presented in Fig. S1-S3. The exhaustive descriptions for the thermal decomposition processes of these radicals are discussed as follows.

As shown from Fig. 2-4, the calculated barriers by using the CCSD(T) (*italic*) method are in qualitative agreement with those from the CBS-QB3 results, although some stationary points have small apart in energy. Thus, in this work, unless otherwise mentioned, the energetic description obtained by CBS-QB3 model chemistry is applied to discuss in the subsequent analysis. As seen from Fig. 2, the barriers for exocyclization processes ($R_{3e\text{-}cis}$, $R_{3e\text{-}trans}$, and R_{3l}) are much lower than that of other pathways, in which the $R_{3e\text{-}cis}$ and $R_{3e\text{-}trans}$ have near identical energies (the difference is 0.25 kcal·mol^{-1}). The barrier heights are attributed to the influence of low strain energy in the cyclic transition states of 1,4-vinyl migration reactions, which will be discussed detailedly in the following paragraph.

The initial steps of 2-Me-cyclohexyl radical pyrolysis include three pathways: the ring opening R_{3a} (C5-C6 bonds cleavage produces 4-Me-5-C_6H_{10}-1), R_{3i} (C2-C3 bonds scission forms 5-C_7H_{13}-1), and CH_3-elimination R_{3m} (leads to c-C_6H_{10} + CH_3). These processes are accompanied by the barrier heights lies 27.77, 27.13 and 29.84 kcal·mol^{-1} above the total energy of the reactant. The result shows that the C-C bond cleavage on the ring is more advantage than that of the side chain. In the viewpoint of geometrical structures TS3a, TS3i and TS3m, as showed in Fig. S3, the breaking C-C bond is elongated by 50.9, 48.0 and 46.2%, whereas the forming C=C bond lengths are 1.330, 1.332 and 1.333 Å, respectively, compared to the equilibrium structure calculated for 2-Me-cyclohexyl radical. Therefore, these three transition states are late and product-like, and these reactions with the high energy barrier, strong endothermic (~ 22 kcal·mol^{-1}) and nonspontaneous (11-18 kcal·mol^{-1}), which are coincide with the Hammond's postulate.[35]

The 4-Me-5-C_6H_{10}-1 radical formed by channel R_{3a}, not only produces 2-Me-3-C_4H_6-1 + C_2H_4 (*via* TS3b) by the beta C-C bond scission with a barrier of 28.20 kcal·mol^{-1}, but also forms 2-Me-c-C_5H_8-CH_2-cis/trans radicals (*via* 1,4-vinyl migration TS3e-cis/trans) through a five-membered transition state with the barriers of 8.09 and 7.84 kcal·mol^{-1}. The energies of these two transition states are almost equivalent, meaning that these two reactions play an equal importance in the title reactions. Moreover, the channels $R_{3e\text{-}cis}$ and $R_{3e\text{-}trans}$ are strongly exothermic and spontaneous. The result shows that the 1,4-vinyl migration reactions are thermodynamically and kinetically favored. Then the 2-Me-3-C_4H_6-1 radical in turn dissociates to 1,3-C_4H_6 + CH_3 (*via* TS3c) or C_3H_6 + C_2H_3 (*via* TS3d). These two reactive processes accompany with the barriers of 26.04 and 35.39 kcal·mol^{-1}, respectively. Channel R_{3c} is kinetically more favorable than the R_{3d}, which is attributed to the effect of the breaking C-C bond is in conjunction with a C=C double bond.

The ultimate products of 2-Me-c-C_5H_8-CH_2-cis/trans radical are 1,3-C_4H_6 + C_3H_6 + H through a series of reactions (2-Me-c-C_5H_8-CH_2-cis/trans→R_{3f}→R_{3g}→R_{3h}→ 1,3-C_4H_6 + C_3H_6 + H). These processes accompany with the barriers of 20.74, 20.58,

28.20, 31.66 kcal·mol^{-1}, respectively. The most barrier height is H-elimination process by the cleavage of the strong C-H bond (R_{3h}), whereas the lowest barrier is the ring opening ($R_{3f\text{-}cis}$ or $R_{3f\text{-}trans}$) reaction by C1-C2 bond breaking. It is implied that R_{3h} is the rate limiting step and is thus expected to be a minor decomposition channel. The H-elimination exhibits larger activation energies than the beta C-C bond cleavage (owing to the high bond dissociation energy (BDE) of C-H bond breaking and the stability of products formed). The conclusion is supported by the previous studies.[4,36] Equivalent to the 4-Me-5-C_6H_{10}-1 radical decomposition, the 5-C_7H_{13}-1 radical formed by channel R_{3i}, also has two reactive channels. One is to product 1-C_3H_5-1 + 2C_2H_4 by two consecutive C-C bond scission reactions (R_{3j} and R_{3k}) with the barriers of 27.93 and 35.95 kcal·mol^{-1}, respectively. Another is to form 2-Me-c-C_5H_8 through 1,4-vinyl transfer rearrangement (R_{3l}) with a barrier of 7.52 kcal·mol^{-1}. The result confirms the above conclusion again that 1,4-vinyl transfer is kinetically favored.

Just like in the case of the thermal decomposition of 2-Me-cyclohexyl radical, the detailed mechanism of 2-Me-cyclopentyl and 2-Me-cyclobutyl radicals also include the ring opening, exocyclization and the beta C-C bond scission processes. As can be seen from Fig. 3, the most favored channels are 1,3-vinyl transfer rearrangement ($R_{2c\text{-}cis}$, $R_{2c\text{-}trans}$ and R_{2h}) through a four-membered ring transition state. Similar conclusion is also drawn in the processes of 2-Me-cyclobutyl radical pyrolysis (See Fig. 4) that 1,2-vinyl migrate rearrangement ($R_{1d\text{-}cis}$, $R_{1d\text{-}trans}$ and R_{1i}) reactions are dominated through a three-membered ring transition state. To avoid redundancy, we will not be discussed in detail for these two radicals decomposition. In addition, we also compare the barrier heights for 1,4-, 1,3- and 1,2-vinyl migrate rearrangement reactions, which proceed by five-, four- and three-membered ring transition state structures. The calculation shows that the barrier heights decrease in the order of 1,3- > 1,2- > 1,4-vinyl transfer, and the largest difference among them is amount to 7.79 kcal·mol^{-1}. Our viewpoint is also supported by recent literature reports.[10]

As a result, the cis and trans transition states with energies very close to each other. Same conclusion is also drawn in cis and trans isomers. The exocyclization

process is the most favored channel among all of elementary reactions due to lower barrier and high exothermic. The reaction barrier heights for the distinct reaction channels decrease in the order of 1,3- > 1,2- >1,4-vinyl rearrangement.

3.3 Rate coefficients and branching ratios

Table 2 summarizes the modified three parameters Arrhenius expressions of rate coefficients of every elementary reaction involved in the processes of 2-Me-cyclohexyl radical pyrolysis. Other rate coefficients Arrhenius expressions incorporated in 2-Me-cyclobutyl and 2-Me-cyclopentyl radicals are presented in Table S4 and S5, respectively. The computations are done by employing conventional transition state theory together with an asymmetric Eckart tunneling correction based on the energies derived from the CBS-QB3 level of theory, in the temperature range from 500 to 2500 K. Each dihedral angle of both reactant and transition state is investigated using the 1-D hindered rotor treatment. Fig. 5 shows an example of the hindrance potential for an internal rotor, obtained by relaxed potential energy scan with the step of 12° at the B3LYP/6-311G(2d,d,p) level. Fig. 6 presents the Arrhenius plots of rate coefficients for reactions of R_{3c} and R_{3h}, compared with available theoretical results.

From Fig. 6(a) we can see the rate coefficients of the beta C-C bond scission reaction R_{3c} linearly increase with rising temperature, and they satisfy Arrhenius behavior in the whole temperature range. The rate coefficients, both corrected (TST/Eckart) and uncorrected (TST) one, are compared over the temperature range of 500-2500 K. The result shows that the rate coefficients are nearly independent on the tunneling effects. The calculated rate coefficients are within one order of magnitude greater than Tsang's theoretical results,[38] which were determined through the solution of the master equation in the processes of n-pentenyl radical decomposition. For example, at 1800 K, the calculated rate coefficients are 6.82×10^{9} (TST) and 7.14×10^{9} s^{-1} (TST/Eckart), which are higher than the corresponding theoretical value (1.91×10^{9} s^{-1}) by 3.57 and 3.74 times, respectively. Such discrepancy between the computational values and the corresponding literature ones is acceptable.

As seen from Fig. 6(b), for C-H bond cleavage reaction R_{3h}, the rate coefficients increase linearly as the temperature increases, and they also obey positive temperature dependence. The calculated rate coefficient, the agreement with the theoretical data of Weissman et al[37] at 1260-1310 K is quite satisfactory. For example, at 1300 K, the calculated values, 2.25×10^{8} s^{-1}, is quantitatively comparable with the corresponding literature value (4.50×10^{7} s^{-1}). In the following discussion, the theoretical rate coefficients with tunneling effect corrections are applied to discuss the thermal decomposition of 2-Me-cyclohexyl radical.

According to our computations, the rate coefficients of the ring closure reactions $R_{3e\text{-}cis}$ and $R_{3e\text{-}trans}$ are dramatically higher than that of the ring opening pathways $R_{3f\text{-}cis}$ and $R_{3f\text{-}trans}$. Thus, we assume the intermediate 2-Me-C_5H_8-CH_2 radical quickly equilibrates with the free reactants. According to the quasi-steady state approximation (QSSA), the rate coefficient of the formation of 6-C_7H_{13}-2 radical leads to the following expression as eq 4.

$$k = \frac{k_{3e} \times k_{3f}}{k_{-3e} + k_{3f}} \tag{4}$$

where k_{3e} and k_{-3e} are forward and reverse rate coefficients from reactant 4-Me-5-C_6H_{10}-1 to intermediate 2-Me-C_5H_8-CH_2, respectively. k_{3f} is the forward rate coefficient from 2-Me-C_5H_8-CH_2 to 6-C_7H_{13}-2 radical. Similar methodology is adopted to calculate the total rate coefficients of the formation of final products, followed by the branching ratios being estimated at different temperatures. Same computational approach is employed to predict the thermal decomposition of 2-Me-cyclopentyl and 2-Me-cyclobutyl radicals. Fig. 7 displays a graph of the correction between the branching ratios for these radicals against temperatures.

As shown in Fig. 7, the temperature changes have a significant influence on the branching ratio. From Fig. 7 (a) we can see the branching ratio of 2-C_2H_5-c-C_5H_8 radical reduce rapidly at 500-1800 K (from 69.36% to 7.98%), whereas the c-C_6H_{10} + CH_3 exceeds gradually it with the temperature rising (> 1050 K), and they amount to as much as 79.13% at 2500 K. It is concluded that this reaction channel could be

overwhelmingly competitive comparing with other pathways at elevated temperatures. The branching ratio of 3-C_4H_7-1 + C_3H_6 passes through a maximum point with an increase in temperature, and the maximum value is 10.79% (at 750 K). The character is in good agreement with the feature of consecutive reactions. The branching ratios of other routes not exceed 9.0% throughout the entire temperature range, meaning that these pathways can be negligible under normal pyrolysis conditions.

As can be seen from Fig. 7 (b) and (c), the similar conclusions can be drawn in the thermal decomposition of 2-Me-cyclopentyl and 2-Me-cyclobutyl radicals. The branching ratios of c-C_5H_8 + CH_3 (see Fig. 7 (b)) and c-C_4H_6 + CH_3 (see Fig. 7 (c)) exceed gradually 2-C_2H_5-c-C_4H_6 (> 800 K) and 2-C_2H_5-c-C_3H_4 (> 1500 K), and these channels are significantly favoured at high temperature. As above discussion, it is found that the vinyl rearrangement reactions have a significant superiority at low temperature, whereas the formation of cylcoalkenes is favoured at high temperature.

To summarize, firstly, the tunneling effect for the calculation of rate coefficients in all of consideration reactive types is almost no influence in the entire temperature range. Secondly, the 1,2-, 1,3- and 1,4-vinyl rearrangement reactions are more advantaged at low temperature, while the formations of cycloalkene are favored at high temperature. Thirdly, the main products of the thermal decomposition of 2-Me-cyclohexyl, 2-Me-cyclopentyl and 2-Me-cyclobutyl radicals are c-C_6H_{10}, c-C_5H_8 and c-C_4H_6 under normal pyrolysis conditions.

4. Conclusions

In the present works, the thermal decomposition of 2-Me-cyclohexyl, 2-Me-cyclopentyl and 2-Me-cyclobutyl radicals have been investigated thoroughly from the geometries, thermodynamic and kinetic points of view. The following conclusions may be drawn.

(1) The reaction mechanism of the pyrolysis of cyclic alkyl radicals mainly incorporates the ring opening, vinyl rearrangements (exocyclization), beta site C-C bond cleavage and H-elimination processes.

(2) All investigated exocyclization reactions are exothermic and spontaneous,

while the ring opening, C-C bond scission and H-elimination processes are endothermic and nonspontaneous.

(3) The reaction barrier heights for the distinct reaction channels decrease in the order of 1,3-vinyl > 1,2-vinyl > 1,4-vinyl rearrangements.

(4) The vinyl rearrangement reactions are advantaged at low temperature, while the formations of cycloalkene are favored at high temperature.

Acknowledgments

This work was supported by the National Natural Science Foundation of China (No: 21173139, 21473108), the Fundamental Research Funds for the Central Universities (GK: 201101004, 201303004) and Shaanxi Innovative Team of Key Science and Technology (2013KCT-17)

References

1. C. K. Westbrook, W. J. Pitz, O. Herbinet, H. J. Curran and E. J. Silke, *Combust. Flame,* 2009, **156,** 181-199.

2. J. X. Ding, L. Zhang, Y. Zhang and K. L. Han, *J. Phys. Chem. A,* 2013, **117,** 3266-3278.

3. M. R. Zeng, W. H. Yuan, Y. Z. Wang, W. X. Zhou, L. D. Zhang, F. Qi and Y. Y. Li, *Combust. Flame,* 2014, **161,** 1701-1715.

4. B. Sirjean, P. A. Glaude, M. F. Ruiz-Lopèz and R. Fournet, *J. Phys. Chem. A,* 2008, **112,** 11598-11610.

5. J. P. Orme, H. J. Curran and J. M. Simmie, *J. Phys. Chem. A,* 2006, **110,** 114-131.

6. B. Sirjean, P. A. Glaude, M. F. Ruiz-Lopèz and R. Fournet, *J. Phys. Chem. A,* 2006, **110,** 12693-12704.

7. S. Zeppieri, K. Brezinsky and I. Glassman, *Combust. Flame,* 1997, **108,** 266-286.

8. H. J. Curran, P. Gaffuri, W. J. Pitz and C. K. Westbrook, *Combust. Flame,* 1998, **114,** 149-177.

9. H. J. Curran, P. Gaffuri, W. J. Pitz and C. K. Westbrook, *Combust. Flame,* 2002, **129,** 253-280.

10. Z. H. Wang, L. D. Zhang and F. Zhang, *J. Phys. Chem. A,* 2014, **118,** 6741-6748.

11. M. J. Frisch, G. W. Trucks, H. B. Schlegel, G. E. Scuseria, M. A. Robb, J. R. Cheeseman et al (2004) Gaussian 09, revision D.01. Gaussian, Inc., Wallingford.

12. J. Tirado-Rives and W. L. Jorgensen, *J. Chem. Theory Comput.,* 2008, **4,** 297-306.

13. L. L Ye, F. Zhang, L. D. Zhang and F. Qi, *J. Phys. Chem. A*, 2012, **116,** 4457-4465.

14. B. Sirjean, E. Dames, H. Wang and W. Tsang, *J. Phys. Chem. A,* 2012, **116,** 319-332.

15. B. Sirjean and R. Fournet, *J. Phys. Chem. A,* 2012, **116,** 6675-6684.

16. F. Wang, D. B. Cao, G. Liu, J. Ren and Y. W. Li, *Theor. Chem. Acc.,* 2010, **126,** 87-98.

17. C. Gonzalez and H. B. Schlegel, *J. Chem. Phys.,* 1989, **90,** 2154-2161.

18. C. Gonzalez and H. B. Schlegel, *J. Phys. Chem.,* 1990, **94,** 5523-5527.

19. M. Page, *J. Chem. Phys.,* 1988, **88,** 922-935.

20. K. Fukui, *Acc. Chem. Res.,* 1981, **14,** 363-368.

21. J. A. Montgomery, M. J. Frisch, J. W. Ochterski and G. A. Petersson, *J. Chem. Phys.,* 1999, **110,** 2822-2827.

22. A. D. Becke, *J. Chem. Phys.*, 1993, **98,** 5648-5652.

23. G. P. Wood, L. Radom, G. A. Petersson, E. C. Barnes and M. J. Frisch, *J. Chem. Phys.,* 2006, **125,** 094106-16.

24. S. Snitsiriwat and J. W. Bozzelli, *J. Phys. Chem. A,* 2013, **117,** 421-429.

25. J. Mendes, C. W. Zhou and H. J. Curran, *J. Phys. Chem. A,* 2013, **117,** 4515-4525.

26. J. Mendes, C. W. Zhou and H. J. Curran, *J. Phys. Chem. A,* 2013, **117,** 14006-14018.

27. B. C. Garrett and D. G. Truhlar, *J. Phys. Chem.,* 1979, **83,** 2921-2926.

28. C. Eckart, *Phys. Rev.,* 1930, **35,** 1303-1309.

29. H. S. Johnston and J. Heicklen, *J. Phys. Chem.,* 1962, **66,** 532-533.

30. J. Mendes, C. W. Zhou and H. J. Curran, *J. Phys. Chem. A,* 2014, **118,** 12089-12104.

31. C. Y. Lin, E. I. Izgorodina and M. L. Coote, *J. Phys. Chem. A,* 2008, **112,** 1956-1964.

32. W. T. Duncan, R. L. Bell and T. N. Truong, *J. Comput. Chem.,* 1998, **19,** 1039-1052.

33. A. Shenghur, K. H. Weber, N. D. Nguyen, W. Sontising and F. M. Tao, *J. Phys. Chem. A,* 2014, **118,** 11002-11014.

34. A. Kossiakoff and F. O. Rice, *J. Am. Chem. Soc.,* 1943, **65,** 590-595.

35. G. S. Hammond, *J. Am. Chem. Soc.,* 1955, **77,** 334-338.

36. J. Z. Ding, L. Zhang and K. L. Han, *Combust. Flame,* 2011, **158,** 2314-2324.

37. M. Weissman and S. W. Benson, *Int. J. Chem. Kinet.,* 1984, **16,** 307-333.

38. W. Tsang, *J. Phys. Chem. A,* 2006, **110,** 8501-8509.

Table 1 Thermodynamic data (kcal·mol^{-1}) of 2-Me-cyclohexyl radical at the CBS-QB3 level

Channels	$\Delta_r H^0_{298}$		$\Delta_r G^0_{298}$
	Cal	Ref	Cal
2-CH_3-cyclohexyl → 4-CH_3-5-C_6H_{10}-1 (R_{3a})	21.53		17.52
4-CH_3-5-C_6H_{10}-1 → 2-CH_3-3-C_4H_6-1 + C_2H_4 (R_{3b})	22.34		11.40
2-CH_3-3-C_4H_6-1 → 1,3-C_4H_6 + CH_3 (R_{3c})	18.61	17.52[a]	8.02
2-CH_3-3-C_4H_6-1 → C_3H_6 + C_2H_3 (R_{3d})	32.40	32.54[a]	20.94
4-CH_3-5-C_6H_{10}-1 → 2-CH_3-c-C_5H_8-CH_2 ($R_{3e\text{-}cis}$)	-15.74		-13.14
4-CH_3-5-C_6H_{10}-1 → 2-CH_3-c-C_5H_8-CH_2 ($R_{3e\text{-}trans}$)	-15.80		-13.29
2-CH_3-c-C_5H_8-CH_2 → 6-C_7H_{13}-2 ($R_{3f\text{-}cis}$)	13.85		10.76
2-CH_3-c-C_5H_8-CH_2 → 6-C_7H_{13}-2 ($R_{3f\text{-}trans}$)	13.91		10.91
6-C_7H_{13}-2 → 3-C_4H_7-1 + C_3H_6 (R_{3g})	23.30		11.95
3-C_4H_7-1 → 1,3-C_4H_6 + H (R_{3h})	28.82	28.67[a]	22.61
2-CH_3-cyclohexyl → 5-C_7H_{13}-1 (R_{3i})	20.22		16.07
5-C_7H_{13}-1 → 3-C_5H_9-1 + C_2H_4 (R_{3j})	21.80	20.44[a]	11.61
3-C_5H_9-1 → 1-C_3H_5-1+ C_2H_4 (R_{3k})	34.40		23.56
5-C_7H_{13}-1 → 2-C_2H_5-c-C_5H_8 (R_{3l})	-15.45		-13.76
2-CH_3-cyclohexyl → c-C_6H_{10} + CH_3 (R_{3m})	23.21	24.47[a]	11.16

[a] are the theoretical values taken from references[4,5]

The ring opening reactions include R_{3a}, R_{3f} and R_{3i}; exocyclization reaction contain R_{3e} and R_{3l}; H-elimination reactions is R_{3h}; the C-C bond scission are remain reactions

Table 2 The theoretical rate coefficients expression of 2-CH_3-cyclohexyl radical pyrolysis

Reactions	log *A*	*n*	E_a/R	Reactions	log *A*	*n*	E_a/R
2-CH_3-cyclohexyl → 4-CH_3-5-C_6H_{10}-1 (R_{3a})	12.86	0.33	13232	4-CH_3-5-C_6H_{10}-1 → 2-CH_3-3-C_4H_6-1 + C_2H_4 (R_{3b})	12.80	0.23	13719
2-CH_3-3-C_4H_6-1 → 1,3-C_4H_6 + CH_3 (R_{3c})	11.91	0.29	12478	2-CH_3-3-C_4H_6-1 → C_3H_6 + C_2H_3 (R_{3d})	13.76	0.23	17203
4-CH_3-5-C_6H_{10}-1 → 2-CH_3-c-C_5H_8-CH_2 ($R_{3e\text{-}cis}$)	10.64	0.02	3917	4-CH_3-5-C_6H_{10}-1 → 2-CH_3-c-C_5H_8-CH_2 ($R_{\text{-}3e\text{-}cis}$)	12.69	0.19	11070
4-CH_3-5-C_6H_{10}-1 → 2-CH_3-c-C_5H_8-CH_2 ($R_{3e\text{-}trans}$)	10.80	0.02	3763	4-CH_3-5-C_6H_{10}-1 → 2-CH_3-c-C_5H_8-CH_2 ($R_{\text{-}3e\text{-}trans}$)	12.85	0.18	10999
2-CH_3-c-C_5H_8-CH_2 → 6-C_7H_{13}-2 ($R_{3f\text{-}cis}$)	12.61	0.14	10037	2-CH_3-c-C_5H_8-CH_2 → 6-C_7H_{13}-2 ($R_{3f\text{-}trans}$)	12.70	0.13	9969
6-C_7H_{13}-2 → 3-C_4H_7-1 + C_3H_6 (R_{3g})	13.16	0.26	13755	3-C_4H_7-1 → 1,3-C_4H_6 + H (R_{3h})	11.04	0.64	13910
2-CH_3-cyclohexyl → 5-C_7H_{13}-1 (R_{3i})	13.07	0.29	12951	5-C_7H_{13}-1 → 3-C_5H_9-1 + C_2H_4 (R_{3j})	13.22	0.25	13551
3-C_5H_9-1 → 1-C_3H_5-1+ C_2H_4 (R_{3k})	13.88	0.19	17732	5-C_7H_{13}-1 → 2-C_2H_5-c-C_5H_8 (R_{3l})	11.02	0.03	3574
2-CH_3-cyclohexyl → c-C_6H_{10} + CH_3 (R_{3m})	13.50	0.33	14294				

The ring opening reactions include R_{3a}, R_{3f} and R_{3i}; exocyclization reaction contain R_{3e} and R_{3l}; H-elimination reactions is R_{3h}; the C-C bond scission are remain reactions; the unit of s^{-1}

Figure Captions:

Fig. 1 Optimized geometries of all stationary points incorporated in 2-Me-cyclohexyl radical at the B3LYP/6-311G(2d,d,p) level along with the available experimental values (Experimental values are indicated by a superscript a; bond lengths are in angstroms and bond angles are in degrees; red line represents the breaking bond)

Fig. 2 Potential energy profile of the thermal decomposition of 2-Me-cyclohexyl radical at the CBS-QB3 and CCSD(T) (*italic*) levels (the prefix and postfix of the number represent the site of double bond and radical, respectively; the ring opening reactions include R_{3a}, R_{3f} and R_{3i}; exocyclization reaction contain R_{3e} and R_{3l}; H-elimination reactions is R_{3h}; the remain reactions are C-C bond scission; relative energies are given in kcal·mol^{-1})

Fig. 3 Potential energy profile of the thermal decomposition of 2-Me-cyclopentyl radical at the CBS-QB3 and CCSD(T) (*italic*) levels (the prefix and postfix of the number represent the site of double bond and radical, respectively; the ring opening reactions include R_{2a}, R_{2d} and R_{2f}; exocyclization reaction contain R_{2c} and R_{2h}; the remain reactions are C-C bond scission; relative energies are given in kcal·mol^{-1})

Fig. 4 Potential energy profile of the thermal decomposition of 2-Me-cyclobutyl radical at the CBS-QB3 and CCSD(T) (*italic*) levels (the prefix and postfix of the number represent the site of double bond and radical, respectively; the ring opening reactions include R_{1a}, R_{1e} and R_{1g}; exocyclization reaction contain R_{1d} and R_{1i}; the remain reactions are C-C bond scission; relative energies are given in kcal·mol^{-1})

Fig. 5 Potential energy diagram for the internal rotation of the **CH_3-cCH-**·$CH(CH_2)_4$ dihedral angle in 2-Me-cyclohexyl radical

Fig. 6 Arrhenius plots of rate coefficients of the reactions of R_{3c} and R_{3h} are calculated at the CBS-QB3 level of theory along with the literature data from references[37,38]

Fig. 7 The branching rations of 2-Me-cyclohexyl (a), 2-Me-cyclopentyl (b) and 2-Me-cyclobutyl (c) radicals decomposition as a function of temperatures

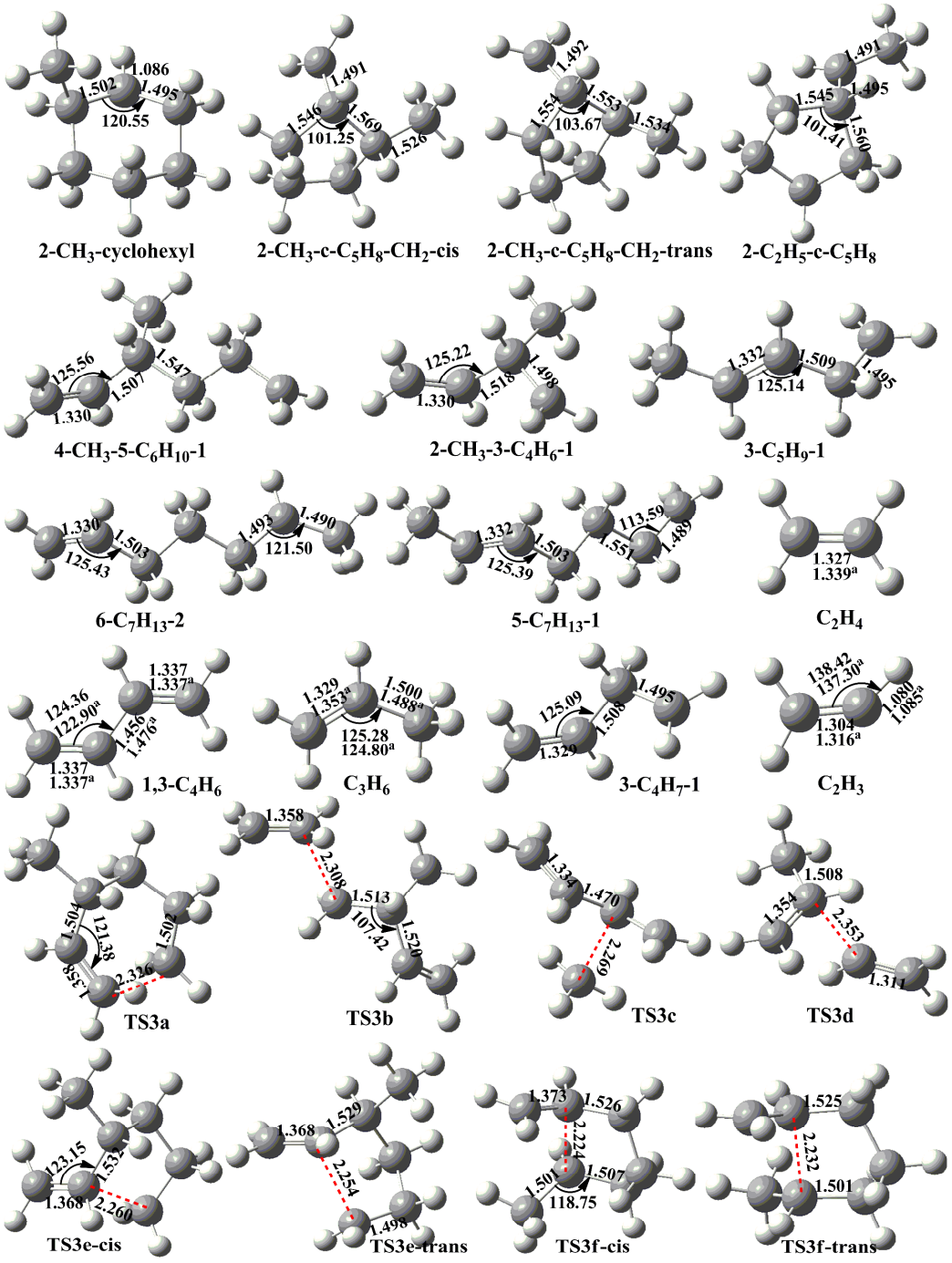

1

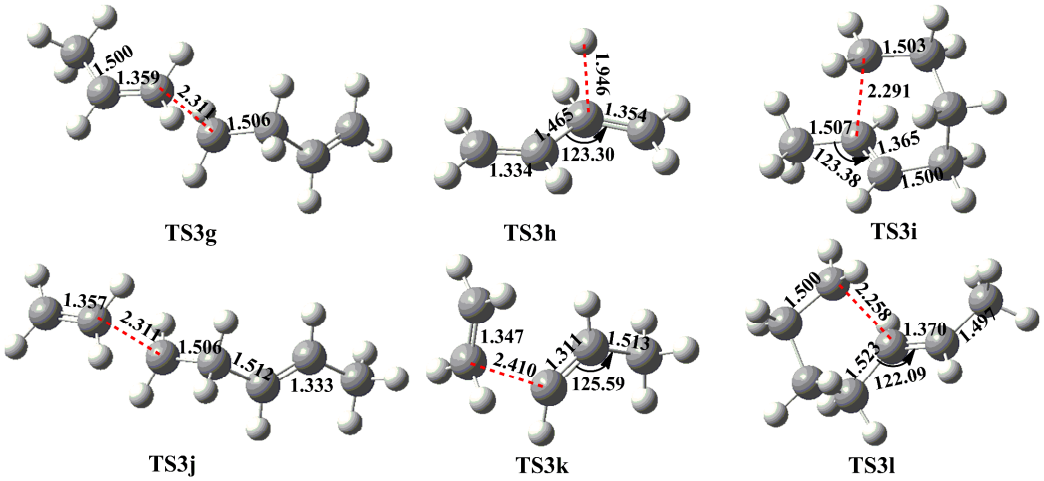

Fig. 1

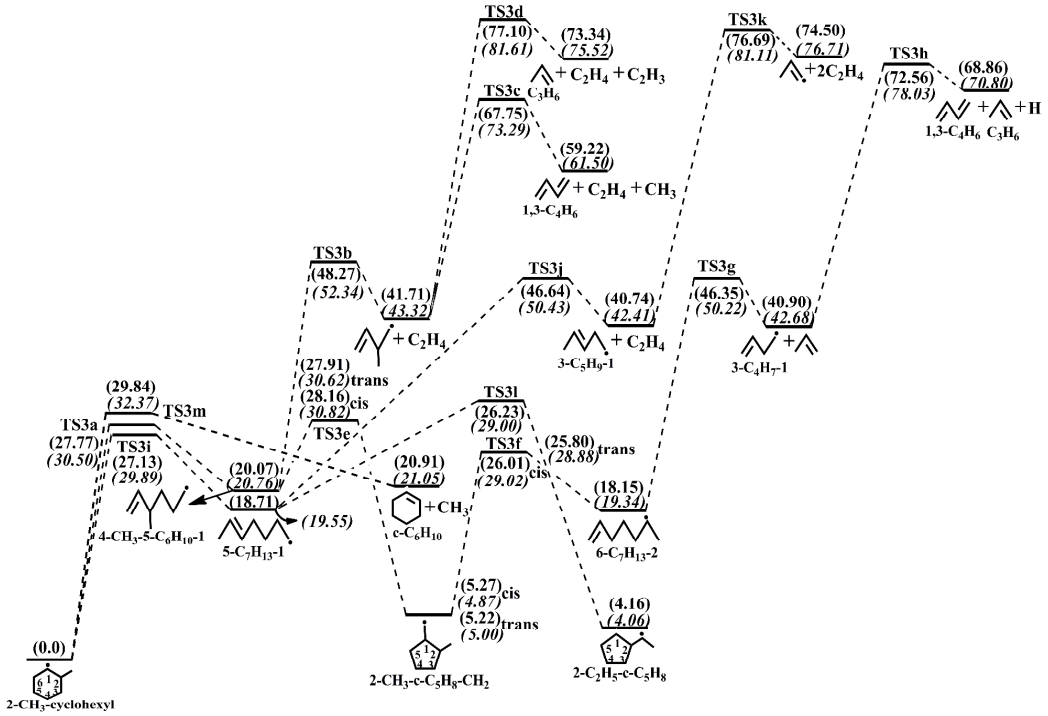

Fig. 2

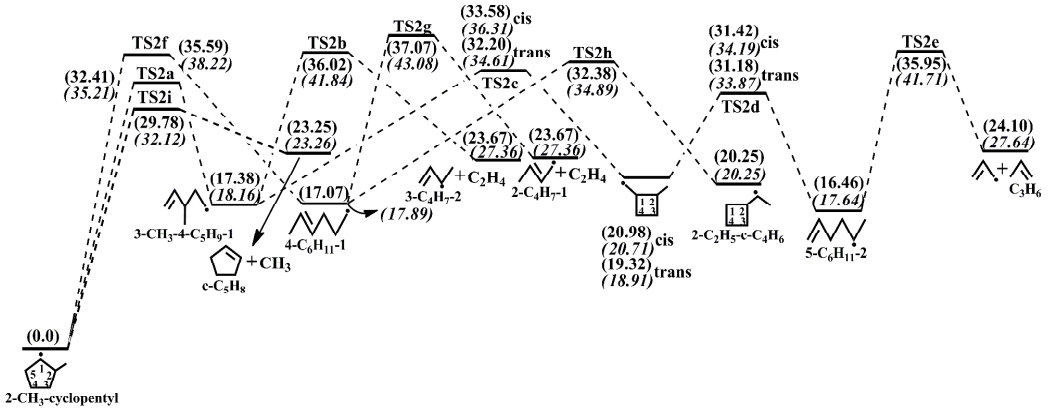

Fig. 3

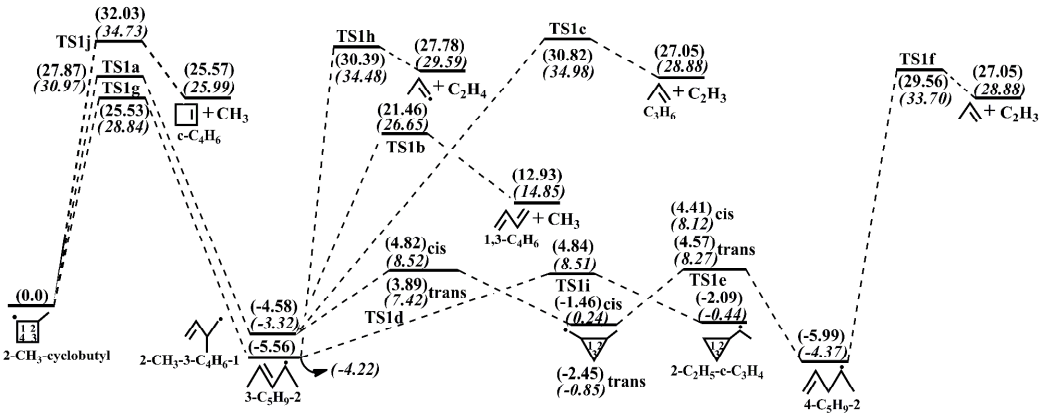

Fig. 4

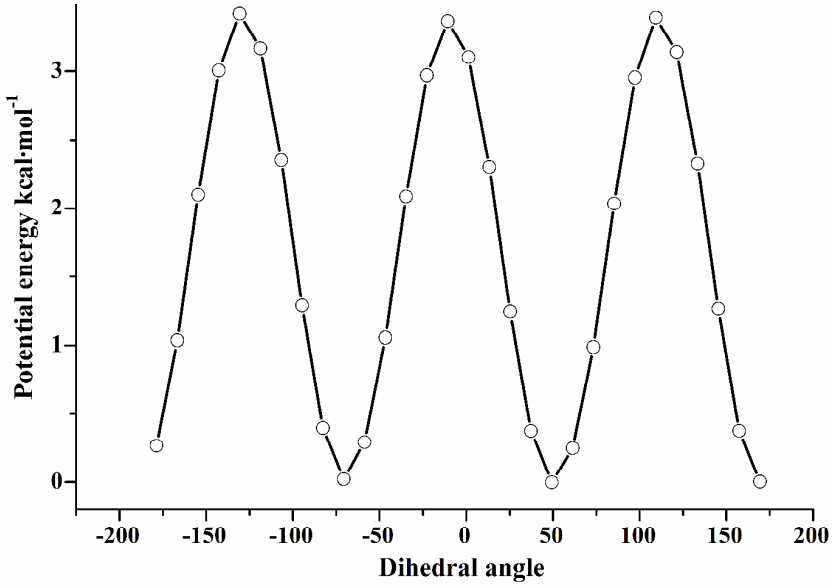

1
2 **Fig. 5**

3

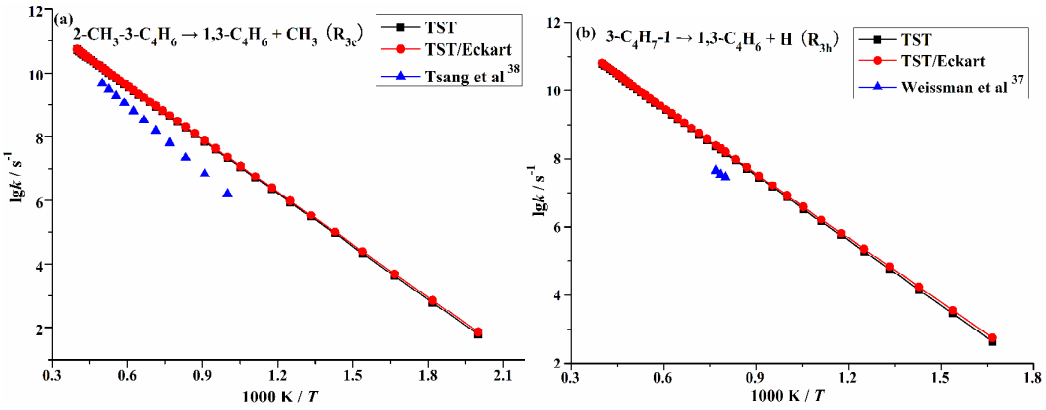

Fig. 6

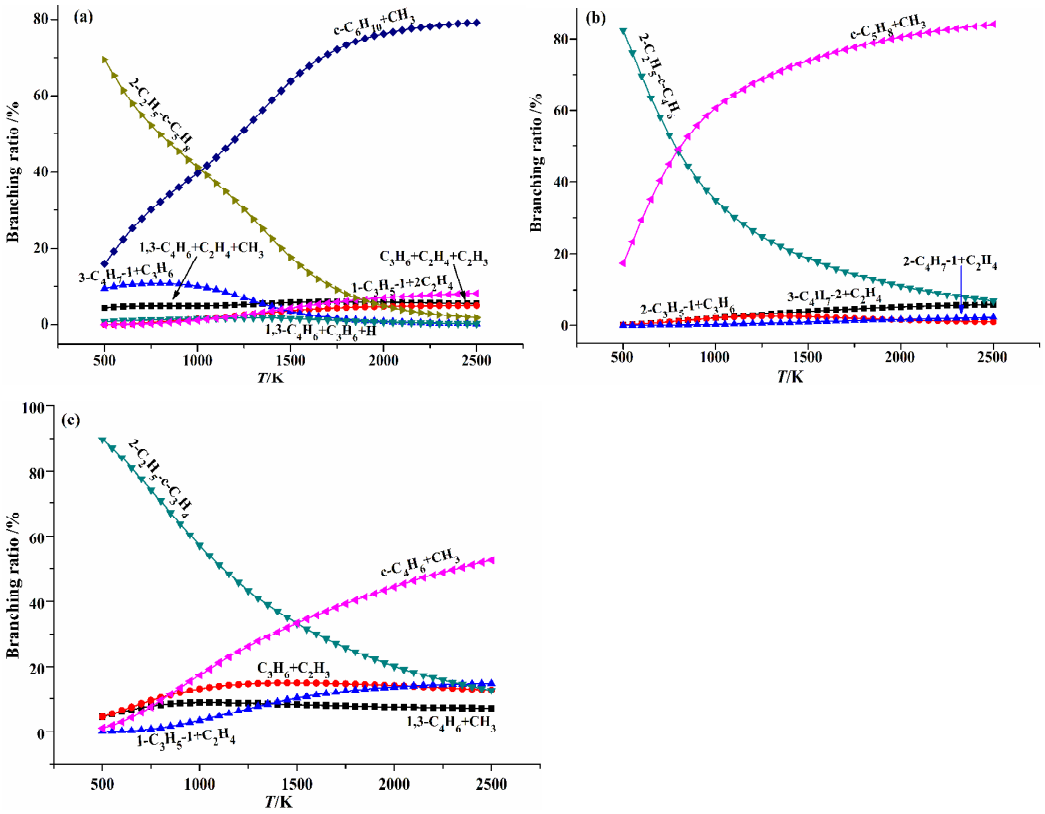

Fig. 7